Received: 6 May 2024 | Revised: 31 July 2024 | Accepted: 29 September 2024

DOI: 10.1002/aic.18621

RESEARCH ARTICLE

Process Systems Engineering

AIChE JOURNAL

Machine learning-aided process design using limited experimental data: A microwave-assisted ammonia synthesis case study

Md Abdullah Al Masud | Alazar Araia | Yuxin Wang | Jianli Hu | Yuhe Tian

Department of Chemical and Biomedical Engineering, West Virginia University, Morgantown, West Virginia

Correspondence
Yuhe Tian, Department of Chemical and Biomedical Engineering, West Virginia University, Morgantown, WV 26506, USA.
Email: yuhe.tian@mail.wvu.edu

Funding information
West Virginia University; West Virginia Science and Research, West Virginia Higher Education Policy Commission, Grant/Award Number: RCG23-009

Abstract

An open research question lies in how machine learning (ML) can accelerate the design optimization of chemical processes which are at very early experimental development stage with limited data availability. As an example, this article investigates the design of an intensified microwave-assisted ammonia production reactor with 46 experimental data. We present an integrated approach of neural networks and synthetic minority oversampling technique to quantify the nonlinear input-output relationships of this process. For ammonia concentration predictions at discrete operating conditions, the approach demonstrates 96.1% average accuracy over other ML methods (e.g., support vector regression 84.2%). The approach has also been applied for continuous optimization, identifying the optimal synthesis conditions at 597.37 K, 0.55MPa with feed flow rate of 1.67 $\times 10^{-3}$ m^3/s kg and hydrogen to nitrogen ratio of 1 which is consistent with experimental observations. The data-driven model enables to integrate this reactor with existing ammonia production infrastructure and benchmark with conventional techniques.

KEYWORDS
machine learning, microwave-assisted ammonia synthesis, neural networks, process design, process intensification

1 | INTRODUCTION

Machine learning (ML) offers a promising strategy to learn the intricate multivariate input-output relationships from large datasets for cost-effective model development. The potential of ML has been extensively demonstrated in chemical process applications such as process design and synthesis, material screening and inverse design, physical property estimation, etc.[1–3] Data-driven models can be generated using the data obtained from plant operations or mechanistic model simulations.[4,5] Hybrid modeling has also gained recent impetus which augments machine learning with mechanistic modeling for mechanism estimation, mechanism correction, physics-informed machine learning, etc.[6,7]

ML requires a significantly large volume of data, generally at the level of thousand, to generate reliable predictions and judgements. For example, the prediction error can be reduced by 20% if doubling the number of training data.[8] Despite well accessible in many engineering applications (e.g., digital twins, automation), data availability presents a formidable challenge for novel chemical process technologies at the very early development stage which typically rely on lab-scale experimental breakthroughs. Due to the time and cost constraints of experimentation, only tens of data may be obtained from a series of experimental tests examining multiple input factors. In addition, experiments are normally run by changing one input factor (or control variable) at a time, as a result of which the data are not well distributed over the input space for machine learning applications. Integrating Design of Experiment with ML was showcased to provide improved modeling performance by generating better distributed experimental samples.[9,10]

Several recent works have explored the use of ML to identify the optimal material or process design conditions based on a limited amount of experimental data. Lih et al.[11] investigated a silicon wafer chemical mechanical planarization (CMR) process with 41 experimental data. An adaptive-network-based fuzzy inference system modeling approach, augmenting the advantages of neural networks (NNs) and fuzzy logic inference system, was developed to quantify the sophisticated nonlinear relationships between the CMR machine and material parameters. Liu et al.[12] addressed the limited data challenge by generating supplemental synthetic data using the synthetic minority oversampling technique (SMOTE).[13,14] An integrated approach was developed utilizing SMOTE-regression, deep NNs, and local interpretable model-agnostic explanations to predict the dimensions of semiconductor carbon nanorods using 28 experimental data. As can be noted, such ML-aided experimental data analysis in particular benefits advanced manufacturing processes which feature complicated physical/chemical behaviors and lack widely accepted mechanistic models. Despite these efforts, a major limitation in existing works lies in that the ML modeling accuracy is only validated against discrete input conditions. Namely, given a single set of experimental input conditions, the output is predicted and compared with experimental measurements. The modeling accuracy against continuous prediction is typically ignored. As an example, Kim et al.[15] showed that even with satisfactory modeling accuracy at discrete points, ML could still capture an opposite or oscillating input-output continuous correlation trend against experimental results. This greatly challenges the use of the resulting ML model in optimization, as it will identify a wrong direction toward optimality.

To address the gap, this article aims to develop a ML-aided modeling approach based on limited experimental data while emphasizing the model validation and application for process design, continuous optimization, and system integration. Inspired by the work of Liu et al.,[12] we leverage the SMOTE oversampling technique to address the challenge of limited data. We demonstrate the use of SMOTE with simple NNs to capture the (nonlinear) input-output relationships, which provides a concise but effective strategy for both discrete and continuous predictions. The proposed approach is applied to study an intensified microwave-assisted ammonia synthesis reactor. Microwave reactors have received increasing research interest in the recent years with well-recognized potential contributing to chemical industry decarbonization and electrification.[16–18] In conventional heating, heat is applied to the reactor externally; however, microwave reactor provides heat to reactant molecules through dielectric heating which leads to the formation of dipoles.[19] The electromagnetic radiation of microwave energy creates an oscillation of polar molecules which results in the heating of molecules. The catalysts are desired to have high dielectric sensitivity in order to absorb the majority of microwave energy.[20,21] The use of microwave thus enables fast and selective heating of the raw materials, creating an alternative path for the reactant molecules to overcome the barrier of high activation energy.[22] Specifically for microwave-assisted ammonia synthesis,[23,24] key advantages have been demonstrated over conventional thermal reactors which include: (i) milder reaction conditions at ambient pressure and lower temperature (around 573–673K), (ii) minimized reverse reaction for ammonia decomposition and improved ammonia productivity, and (iii) less energy consumption. However, the industrial deployment of microwave reactors is yet at an early stage compared to commercial ammonia production processes using the classic Haber-Bosch reactors[25] with high energy and carbon intensity (temperature at 673–773K, pressure above 10MPa).

The modeling and simulation of microwave reactors present another open research question due to their multiphase (e.g., gas-solid), multiphysics (e.g., reaction, electromagnetism), and multiscale nature (e.g., catalyst particle in millimeters to reactors in meters).[26,27] Using the modeling of microwave selective absorption as an example: For a certain type of material, its absorption of microwave heating depends on its dielectric response which can be expressed by the complex permittivity, that is, $\epsilon = \epsilon' + i\epsilon''$. The real component indicates the capability of the material to absorb microwave energy, while the imaginary component reflects its capability to transform the absorbed microwave energy into heat.[28] Two methods can be used to model the microwave power absorption[29]: (i) Lambert's law approximation, and (ii) Maxwell's equation. Lambert's law assumes that microwave power absorption is a function of the penetration depth into the reactor and the absorbed power decreases exponentially as the depth increases. This law only takes the transmission of waves into account but does not consider the reflection of waves. On the other hand, Maxwell's equation considers both the transmission and reflection of waves. Several works applied the Maxwell's equations to describe the microwave selective absorption in catalyst metal particles and coupled the catalyst-level model with the bulk reactor model for microwave-assisted methane dehydroaromatization process, etc.[30–32]

Using the microwave-assisted ammonia synthesis as a representative example, a key challenge lies in the lack of a widely accepted first-principle modeling strategy. This involves a high level of complexity due to the need to accurately simulate the interaction between electromagnetic fields and materials at the atomic level, encompassing both the dielectric properties of materials and their thermal responses. Limitations also remain on, for example, how to more accurately describe the multiscale mass and heat transfer phenomena, how to account for the catalyst degradation dynamics and hot spot formulation which affect the overall reaction performance. The mechanistic modeling also results in large-scale highly nonlinear partial differential algebraic equations or more detailed computational fluid dynamics models which are computationally expensive to solve, thus hindering the further development for process optimization and systems-level evaluation. This article aims to address this challenge by developing an alternative strategy using ML and limited experimental data to systematically model the input-output relationships of a microwave-assisted ammonia synthesis reactor and to rapidly identify the near-optimal reaction design parameters to guide experimental tests even before establishing a rigorous mechanistic model.

The remainder of this paper is organized as follows: Section 2 introduces the microwave reactor of interest with the available experimental data. Section 3 details the proposed SMOTE-integrated NNs approach and its application to model the microwave reactor. Comparisons of the proposed approach with other ML approaches are also discussed such as support vector regression and NNs.

Section 4 showcases the potential of the ML model to enable the evaluation and integration of microwave reactor with existing ammonia production infrastructure. Section 5 presents concluding remarks.

2 | MOTIVATING CASE STUDY: MICROWAVE-ASSISTED AMMONIA SYNTHESIS

In this article, we investigate the microwave-assisted ammonia synthesis reactor developed in Wang et al.[24] A schematic of this reactor is given in Figure 1. Ammonia is produced from hydrogen and nitrogen (both 99.99% purity) as an exothermic reaction. $CsRu/CeO_2$ catalyst is utilized which demonstrates high ammonia synthesis activity under ambient pressure and microwave conditions.[33] Experimental studies are conducted in the original paper to analyze the impact of key process parameters on reactor outlet NH_3 concentration (NH_3%) which include reaction temperature (T), pressure (P), feed gas flow rate (F), and H_2 to N_2 ratio (H_2:N_2). A total of 46 experimental data are available as illustrated by the markers in Figure 2. The trend lines are generated based on the scatter plots while without mathematical regression. As can be noted, the experiments are performed by varying one control variable at a time. The experiments for Figure 2B are designed at the pressure of 0.55MPa and H_2 to N_2 ratio of 1, because this provides the highest ammonia concentration based on Figure 2A. An indicative list of the corresponding data point values is also provided in Table 1. The process parameters are investigated within temperature 553–673K, pressure 0 to 0.55MPa, feed gas flow rate 8.33×10^{-4} to 4.17×10^{-3} $m^3/s\,kg_{cat}$, and H_2 to N_2 ratio 1:2 to 5:1. The range of experimental data determines the maximum design space for the ML modeling to be presented in the following section. To extend the design space (e.g., to examine the NH_3% at $T = 693$K), new experimental data should be supplemented accordingly before applying ML modeling.

The research objectives of this work include:

- Develop a multiple-input single-output data-driven model for this microwave-assisted ammonia synthesis reactor based on the 46 experimental data.
- Optimize the reaction conditions (T, P, F, H_2:N_2) using the resulting ML model to maximize ammonia concentration.
- Prove the concept of utilizing the ML model to evaluate the systems integration of this reactor into existing ammonia production infrastructure accounting for hydrogen production, nitrogen production, etc. and benchmark with Haber-Bosch process within a unified modeling framework.

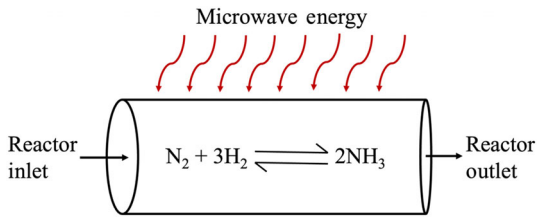

FIGURE 1 A schematic of the microwave-assisted ammonia synthesis reactor.

3 | ML-AIDED PROCESS DESIGN USING EXPERIMENTAL DATA

3.1 | Overview of the methodology

We propose a SMOTE-integrated NNs approach with softplus activation function to generate data-driven input-output models based on a limited amount of experimental data. A flowchart summarizing the steps of SMOTE-integrated NNs is illustrated in Figure 3. SMOTE is used to reliably generate synthetic data points to address the challenge of sparse training data. NNs are employed to capture the typically nonlinear behavior between the input features and the target outputs. Herein, simple NNs are adopted instead of deep NNs to provide sufficient modeling accuracy but with significantly reduced mathematical complexity. This feature is instrumental to enable computational efficiency and tractability when integrating the data-driven model with systems-level optimization to be discussed in Section 4. We also highlight the role of the activation function in generating smooth continuous prediction. The use of soft plus and rectified linear unit activation functions are compared to emphasize the importance of validating continuous prediction in addition to discrete prediction.

The proposed approach also provides a more computationally efficient strategy compared to conventional modeling using large-scale systems of differential algebraic equations.[26,30] First-principle modeling of microwave reactors requires solving Maxwell's equations in conjunction with heat transfer equations, often resulting in computationally intensive simulations to accurately simulate the interaction between electromagnetic fields and materials at the atomic level. There also lacks a well-accepted model for microwave reactors, as the behavior can vary significantly depending on the specific materials, operating conditions, and modeling assumptions.

In what follows, the proposed method is first applied to model the afore-introduced microwave-assisted ammonia synthesis reactor with a step-by-step procedure. After validating the discrete and continuous prediction performances, the resulting data-driven model is leveraged to optimize the reaction conditions for maximum ammonia concentration. Several comparative studies are then presented to justify the superior performance of the proposed method over NNs without SMOTE, support vector regression, etc.

3.2 | Step-wise application to microwave reactor

3.2.1 | SMOTE synthetic data generation

The SMOTE algorithm has been widely applied to solve classification problems for imbalanced datasets.[13,14] The whole dataset is divided into majority class samples and minority class samples. The distinction of

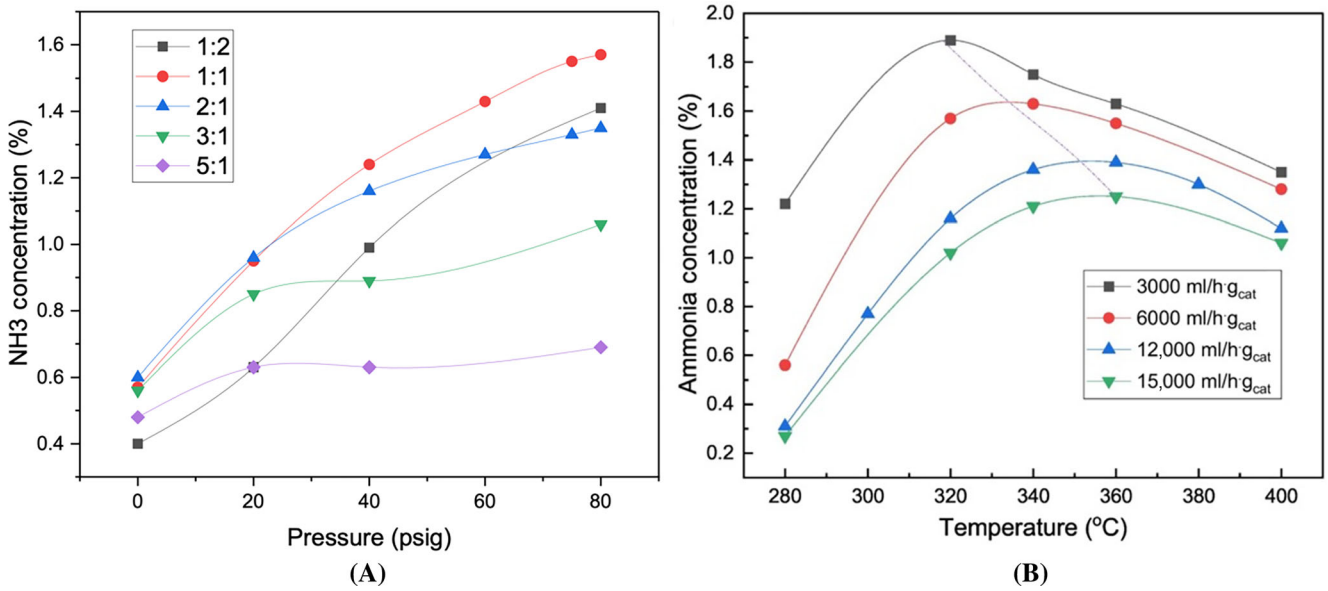

FIGURE 2 Experimental results on the impact of process parameters (reproduced from Wang et al.[24]). (A) $T = 320^\circ$C, $F = 6000$ mL/h g; (B) $P = 80$ psig, $N_2 = 1$.

TABLE 1 Available experimental data — an indicative list.

T (K)	*F* (m^3/s kg_{cat})	H_2:N_2	*P* (MPa)	NH_3%	*P* (MPa)	NH_3%
593	1.67×10^{-3}	1:2	0	0.40	0.28	0.99
		1:1		0.57		1:24
		2:1		0.60		1:16
		3:1		0.56		0:89
		5:1		0.48		0:63
P (MPa)	H2:N2	*T* (K)	*F* (m^3/s kg_{cat})	NH_3%	*F* (m^3/s kg_{cat})	NH_3%
0.55	1	553	1.67×10^{-3}	0.56	4.17×10^{-3}	0.27
		593		1.57		1.02
		613		1.63		1.21
		633		1.55		1.25
		673		1.28		1.06

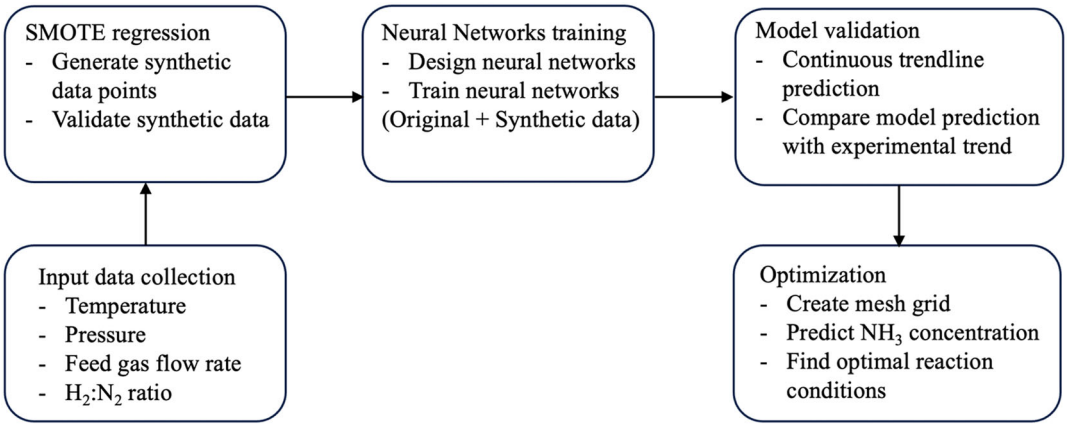

FIGURE 3 Flow diagram of synthetic minority oversampling technique (SMOTE)-integrated neural networks.

majority and minority can be performed using a user defined threshold to screen out the extreme values as minority class. For the values that lie over or under the threshold, SMOTE can generate neighboring instances so that the ratio of majority and minority class samples can be balanced. This oversampling technique is suitable for unbalanced classification problems. The strategy of random oversampling effectively increases the data distribution for the minority class. ML algorithms are typically challenged from learning imbalanced datasets and may thereby perform unsatisfactorily to predict labels for both majority and minority classes. With the additional samples from SMOTE, the ML algorithms can be better trained to provide more accurate and robust classification performance with reduced biases. SMOTE has been later extended for regression tasks which involve continuous data prediction rather than the discrete class labels.[34] The synthetic data points can be generated by the interpolation of feature vectors from the original data.[12]

In this article, SMOTE regression is applied to the 46 experimental data that are obtained from the microwave-assisted ammonia synthesis reactor (Table 1). The key objectives of incorporating SMOTE in our work are to: (i) generate synthetic data points that follow a similar distribution pattern with the original experimental data, (ii) provide sufficient data to the NNs to ensure good training, and (iii) thus improve the discrete and continuous prediction accuracy of ammonia concentration. The synthetic data generation is illustrated in Figure 4 with the major steps summarized below. In our case with the 46 experimental data, any combination of samples can be considered as an extreme value.

i. For a sample y in the minority class, k neighboring samples $\tilde{y}$ are identified and the distances between the sample and the synthetic neighbors are calculated using Euclidean distance.
ii. A fraction η ranging from 0 to 1 is randomly selected for one of the neighboring samples and multiplied by the distance. The product is then added to the minority class sample. The synthetic sample y_{new} is obtained from the following expression:

$$y_{new} = y + \eta \times (y - \tilde{y}). \quad (1)$$

iii. The next step is the merging of synthetic samples with the experimental data points. The iterations continue until a set of desired sample size is obtained.

The same data generation technique is followed for the input and output variables. Using the SMOTE regression, 40,589 new synthetic data points are generated accounting for four input variables (i.e., T, P, F, H_2:N_2) and one output variable (i.e., NH_3%). Before utilizing these data to train the NNs model, it is essential to check the physical validity of the synthetic data. Figure 5 shows the scatter plots of these synthetic data points in terms of pressure, H_2 to N_2 ratio, and NH_3 concentration. As can be noted from Figure 5A, all the NH_3 concentrations lie within 0 to 2% which are consistent with the experimental data. No data points are reported as anomaly (e.g., negative values or substantially high). Figure 5B verifies that the synthetic data are well distributed over the input parameter space.

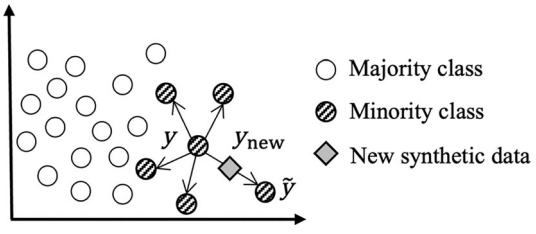

FIGURE 4 Synthetic minority oversampling technique (SMOTE) synthetic data generation.

3.2.2 | Regression via NNs

NNs offer the capability to automatically learn from a dataset and discern the underlying patterns without requiring a complete specification of the decision model.[35,36] NNs model comprises an input layer, several hidden layers, and an output layer. The input layer receives the input features with the hidden layers to perform the data transformation and the output layer to produce the desired output. The output of a particular layer becomes the input of the following layers. In a particular hidden layer, one neuron is connected to every other neuron in the next layers. This mapping of learning helps the model to precisely detect the complex relationships for a multivariate problem.[37] If multiple hidden layers are used, hierarchical feature extraction can be achieved by the networks.[3]

In this article, the NNs model is developed with two hidden layers and 257 neurons for regression between T, P, F, H_2:N_2, and NH_3%. Mean squared error (MSE) is used as the loss function for training. The loss function minimizes the difference between the true values and the predicted values. After each batch operation, the loss value becomes less than the previous one as the model gradually learns better and better. As depicted in Figure 6, each neuron is associated with weights and biases. The hyperparameters are tuned during the training process to best correlate the input and output data following the guidelines in the literature.[38] The learning rate, which dictates the magnitude of weight adjustments relative to the loss gradient, must be carefully chosen; an excessively high learning rate can cause convergence issues, whereas an excessively low rate can lead to slow training. The number of epochs, representing the number of complete passes through the training dataset, requires balance to avoid overfitting or underfitting. Batch size impacts both the stability and speed of the training process, with smaller batch sizes offering more frequent updates and larger batch sizes providing more stable gradient estimates. The number of neurons in each layer determines the model's learning capacity; insufficient neurons may lead to underfitting, while an excessive number can result in overfitting. An activation function is a function of the sum of weights and biases for a neuron, that is, $y^t = f(\sum w^t x^t + b^t)$, which can thus transform the linear combination of inputs into a nonlinear output.[39] This feature enables the NNs model to capture the nonlinear behavior in datasets, which is critical for the microwave-assisted ammonia synthesis reactor of interest. Herein, we compare two commonly used activation functions: (i) rectified linear unit (ReLU), and (ii) softplus.

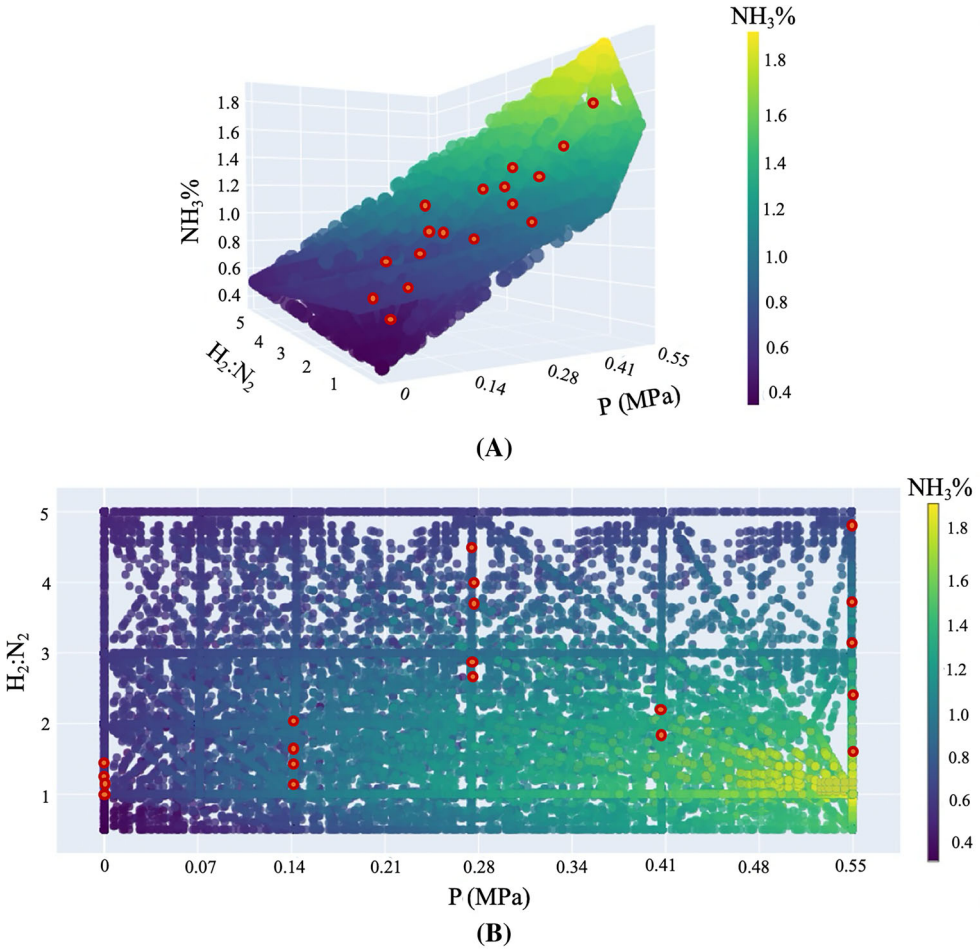

FIGURE 5 Validation of synthetic data from synthetic minority oversampling technique (SMOTE) regression. (A) Synthetic data — 3D scatter plot (Markers: experimental data); (B) Synthetic data — 2D scatter plot (Markers: experimental data).

The ReLU activation function is piece-wise linear and defined as Equation (2). As shown in Figure 6, this function returns zero for any negative inputs while returning the input value for any positive inputs. The softplus activation function is expressed as Equation (3) which always returns a positive value irrespective of the inputs. Based on its mathematical definition, softplus activation function is differentiable at any point. This leads to the observation that softplus can provide a smooth and continuous curve prediction compared to the ReLU activation function.[40] This key advantage over ReLU is due to that softplus does not suffer from the "dying ReLU" problem. This problem refers to the situations in which some neurons in the networks become inactive, therefore not being able to update the corresponding weights and biases and resulting in nonsmooth predictions.

ReLU:

$$f(x) = \begin{cases} x_i & \text{if } x_i > 0 \\ 0 & \text{if } x_i < 0 \end{cases}. \quad (2)$$

Softplus:

$$f(x) = \ln(1 + e^x). \quad (3)$$

The impact of ReLU and softplus on NNs modeling of the microwave-assisted ammonia synthesis reactor is shown in Figure 7. Both activation functions are able to capture the nonlinearity with similar modeling accuracy against the discrete original experimental data points (i.e., markers in Figure 7). However, when validated against the continuous trend, the ReLU NNs model presents notable non-smooth predictions at low pressures (Figure 7A). As of such, softplus is adopted in the remaining of this article for data-driven modeling. This also highlights the importance to validate the continuous predictions of the resulting ML regression models which has been generally neglected in existing works.[11,12,15]

3.2.3 | Regression via other ML methods

The proposed use of NN for regression will be compared with two alternative ML-aided regression approaches, for example, linear regressions and support vector regressions. The basics of these two algorithms are briefly reviewed in what follows.

Linear regressions

Linear regression[41] correlates the input-output relationship in the form of a straight line. The response of the target variable can be interpreted from one or multiple independent variables as expressed in Equation (4). In a multivariate linear regression model, each of the independent variables are associated with coefficients a_i. The ML algorithm

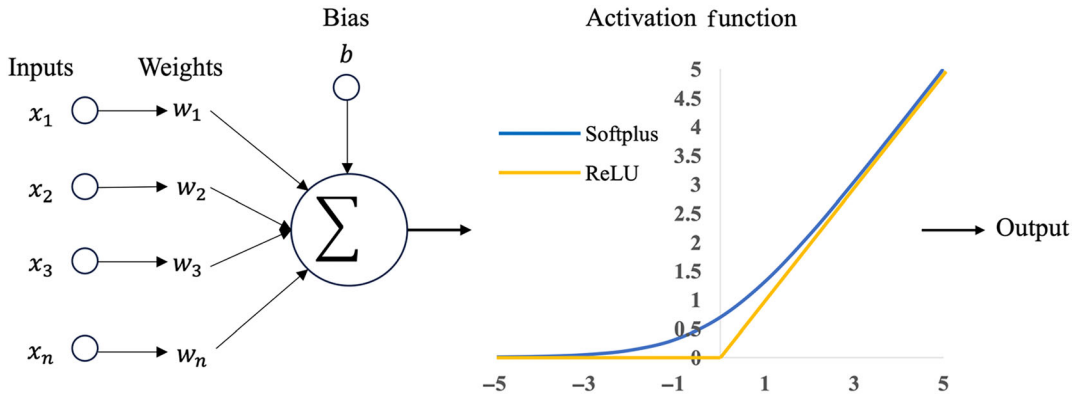

FIGURE 6 A schematic of neural networks and activation functions. Nomenclature: w^t is the matrix for weights, b^t is the matrix for biases, x^t is the input vector for a specific layer, and y^t is the output vector of that layer.

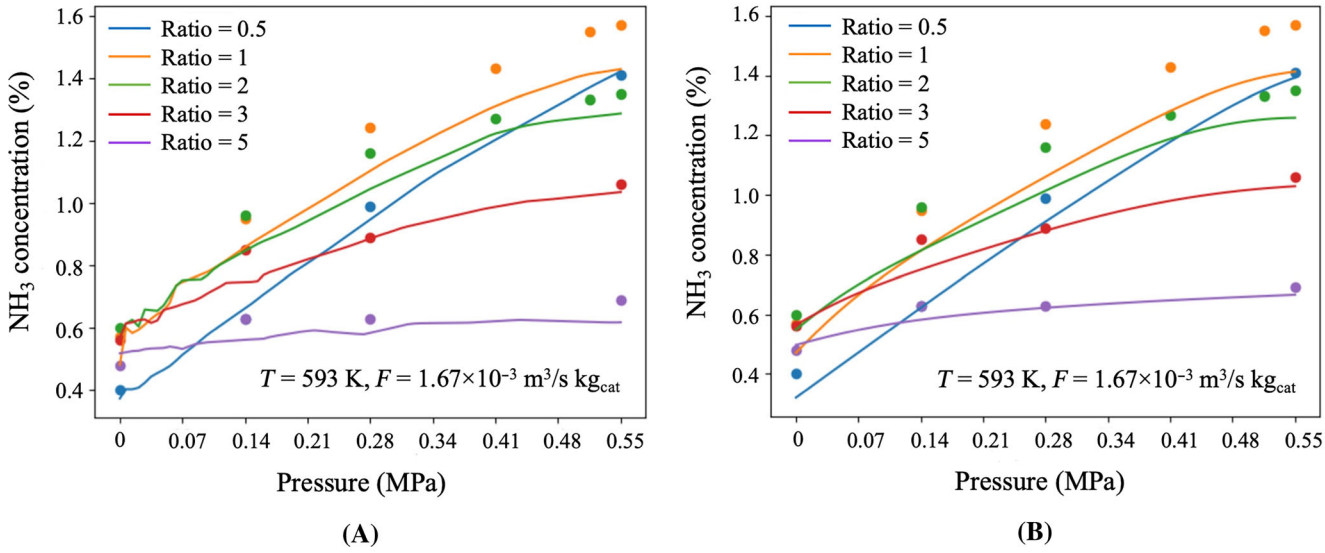

FIGURE 7 Impact of activation function for continuous prediction. Markers: Original experimental data. Lines: synthetic minority oversampling technique (SMOTE)-integrated neural networks modeling. (A) ReLU activation function; (B) Softplus activation function.

tunes these coefficients during the training session so that the model can appropriately fit to the training data and then provide satisfactory prediction accuracy on the unseen datasets. Linear regression is performed to provide a lower bound to benchmark the modeling accuracy of the other ML regression methods, as the input-output relationship of this microwave reactor is expected to be nonlinear.

$$Y = a_0 + a_1X_1 + a_2X_2 + a_3X_3 + a_4X_4 + \ldots, \tag{4}$$

where X represents the input variables, and Y represents the output response. $a_1, a_2, a_3, a_4, \ldots$ are tunable coefficients, and a_0 is the intercept.

Support vector regressions

Support vector regression (SVR)[42] employs a kernal function $f(x)$ with an epsilon intensive loss function (ϵ) to model input-output relationships. Either linear or nonlinear regression can be achieved via the choice of different kernel functions, the role of which is to map the data into higher dimensional spaces. As shown in Figure 13, the commonly used kernel functions are linear kernel, polynomial kernel, radial basis function (RBF) kernel, sigmoid kernel, etc. The mathematical formulation of SVR is presented in Equation (5), from which the hyperparameters are determined to minimize the sum of errors (i.e., objective function) subject to a certain level of tolerance (i.e., constraints).

$$\begin{aligned} \min\ & \frac{1}{2}\|w\|^2 + C\sum_{i=0}^{l}(\epsilon_i + \epsilon_i^*) \\ \text{s.t.}\ & y_i - f(x_i) - b \le (\epsilon + \epsilon_i) \\ & f(x_i) - y_i + b \le (\epsilon + \epsilon_i^*) \\ & \epsilon_i, \epsilon_i^* \ge 0, \end{aligned} \tag{5}$$

where w represents the weight vector, b is the bias, C is a regularization parameter, ϵ_i and ϵ_i^* are the upper and lower error bounds for each data that point out the error tolerance.

3.3 | SMOTE-integrated NNs modeling performance

3.3.1 | Discrete prediction

We first apply the SMOTE-integrated NNs model for discrete prediction. A total of 40,635 data points are used with 80% for training and 20% for testing (46 original experimental data and 40,589 synthetic data). Adam optimizer is utilized with the learning rate as 0.0001. The number of epochs is selected as 100, which indicates that the algorithm iterates through the dataset 100 times during the training process. The average discrete prediction accuracy, R^2 value, and MSE of SMOTE-integrated NN is 96.10%, 0.99, 3.47×10^{-3}, respectively, with an indicative list of prediction results given in Table 2.

3.3.2 | Continuous prediction

On the basis of satisfactory discrete prediction accuracy, we proceed to validate and improve the continuous prediction for this microwave-assisted reaction system. However, overfitting is observed when performing continuous prediction using the above SMOTE-integrated NNs model trained by all the synthetic data points. The overfitting is validated by observing the training and validation accuracy of the trained NNs. The higher training accuracy (close to 100%) over the validation accuracy (80%) indicates that the model fails to generalize on unseen data. In this way, 23,000 data points are randomly selected to retrain the NNs model (including the original experimental data and SMOTE synthetic data). It is necessary to ensure that the randomly selected data are well distributed in the parameter space (T, P, F, H_2:N_2) as there is a probability of the skewness. Skewness refers to the asymmetrical distribution of data points (e.g., majority of data samples concentrated on the left or right side). An alternative strategy is to regenerate the desired number of synthetic data via SMOTE which intrinsically ensures good data distribution. We have verified that the implemented random selection strategy provides similar modeling performance with SMOTE synthetic data regeneration.

The model prediction results are shown in Figure 8, following the same way of presenting the original experimental results for convenient comparison (Figure 2). This model accounts for all the four input variables (T, P, F, H_2:N_2) to predict the output NH_3 concentration. The overall continuous prediction performance is satisfactory as it succeeds in capturing the major trends of the multi-variate impacts on NH_3 concentration. However, slight fluctuations are observed in the continuous prediction such as the change of direction at $P = 0.55$MPa and H_2:$N_2 = 1$. This is due to the lack of more experimental data points at the boundary of operating conditions. The trendline of two-input one-output model is slightly better than the four-input one-output model as the latter comprises more nonlinear relationship between the input variables. It is also key to ensure that the impact of pressure on ammonia synthesis is correctly captured, that is, ammonia concentration increases as the increase of pressure.

The input dimension can be a critical factor impacting the SMOTE-integrated NN modeling performance (e.g., the observed fluctuations). This is because that the four input variables exhibit highly nonlinear multivariate relationship against the output variable, as can be expected for this microwave-assisted ammonia synthesis reactor. To examine this hypothesis, we develop two distinct SMOTE-integrated NNs models at lower input dimension (i.e., two inputs and 1 output). The R^2 and MSE for the two-inputs one-output model are 0.99 and 3.45×10^{-4}, respectively. In comparison, the R^2 and MSE for the four-inputs one-output model are 0.97 and 5.02×10^{-3}.

The continuous prediction performance of the two-inputs one-output models is shown in Figure 9, which is notably better than the four-inputs one-output prediction due to the less sophisticated input-output relationship. More specifically, Model 1 is developed to predict NH_3 concentration only as a function of varying pressures and H_2 to N_2 ratios. Among the total 46 sets of experimental data, 24 experiments are run across the pressure range of 0 to 0.55 MPa, H_2 to N_2 ratio range of 0.50 to 5 with fixed temperature at 593 K and feed flow rate at 1.67×10^{-3} $m^3/s\,kg_{cat}$. 11,340 synthetic data points are generated and then fed to train Model 1. Model 2 is developed to predict

TABLE 2 SMOTE-integrated neural networks.

T (K)	*P* (MPa)	H_2:N_2	*F* ($m^3/s\,kg_{cat}$)	Test data NH_3%	Predicted NH_3%	Accuracy (%)	R^2	MSE
593	0.14	0.50		0.63	0.6275	99.60		
593	0	3		0.56	0.5852	95.50		
593	0.52	1		1.55	1.5470	99.80		
593	0.55	2	1.67×10^{-3}	1.35	1.4455	92.92	0.99	3.47×10^{-3}
593	0	2		0.60	0.6252	95.80		
593	0.28	3		0.89	0.9017	98.68		
593	0.55	3		1.06	1.1115	95.14		
593	0.55	1		1.57	1.4493	95.31		
						Average = 96.10		

Note: Discrete prediction accuracy is calculated based on the combined data points.

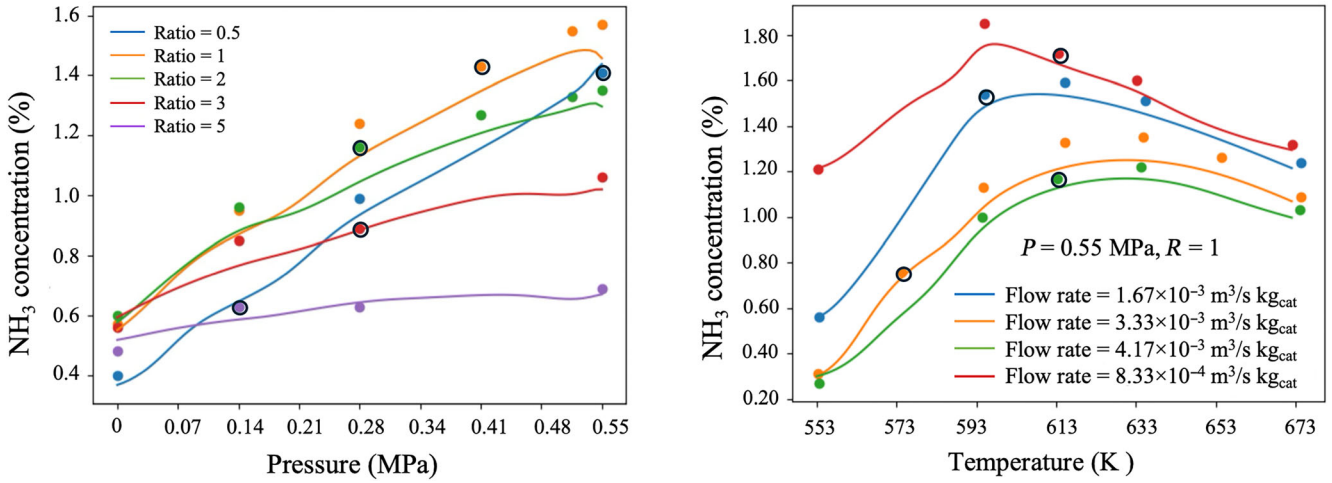

FIGURE 8 Synthetic minority oversampling technique (SMOTE)-integrated neural networks—Continuous prediction (4-input 1-output). Markers: Original experimental data. Circled markers are testing data, and the rest are training data. Lines: SMOTE-integrated neural networks modeling.

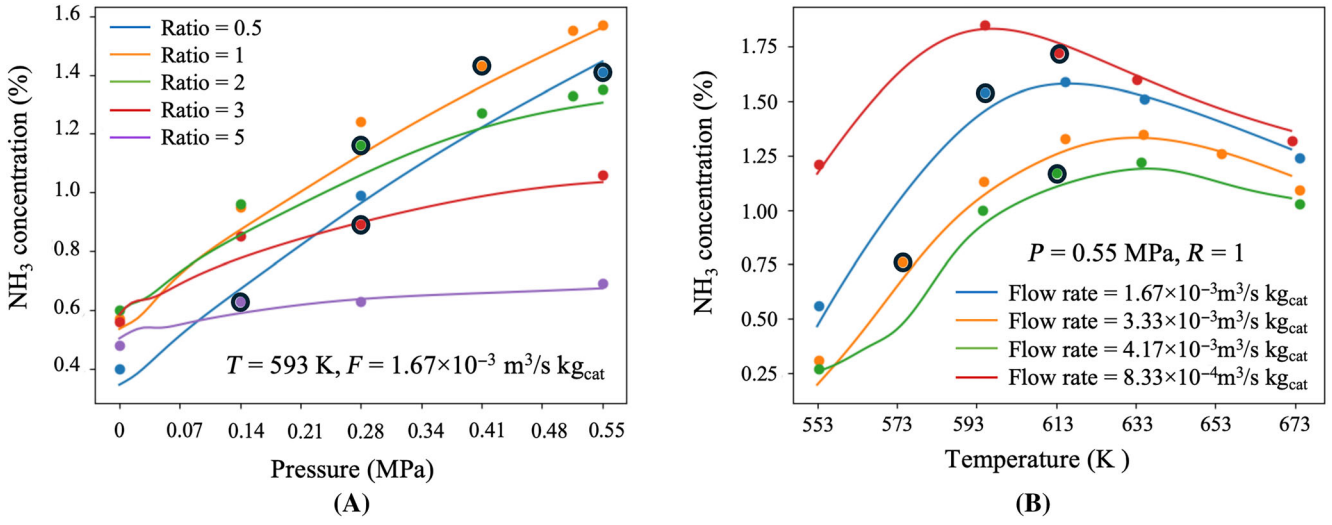

FIGURE 9 Synthetic minority oversampling technique (SMOTE)-integrated neural networks—Continuous prediction (two-input one-output). Markers: Original experimental data. Circled markers are testing data, and the rest are training data, Lines: SMOTE-integrated neural networks modeling. (A) Model 1; (B) Model 2.

NH_3 concentration at different temperatures and feed flow rates. The remaining 22 experiment data are used to generate corresponding synthetic data, which are conducted across the temperature range of 553–673K and feed flow rate range of 8.33×10^{-4} to $4.17 \times 10^{-3}\ m^3/s\ kg_{cat}$ with fixed pressure at 0.55 MPa and H_2 to N_2 ratio at 1. 4,180 synthetic data points are generated and then fed to train Model 2.

3.4 | Design optimization

A key advantage offered by the resulting SMOTE-integrated NNs model is to quantitatively identify the optimal reaction conditions for the highest NH_3 concentration. As illustrated in Figure 10, a simulation-based grid search and optimization strategy is adopted. Rigorous mathematical programming-based optimization is to be introduced in Section 4. Given the reaction design space defined by the experimental data span, a mesh grid is first created. The choice of step size can be tailored to the desired level of accuracy. Herein, the step sizes for T, P, F, and H_2:N_2 are respectively chosen as 1.17, 1, 6000, and 10. Therefore, the total number of data in the mesh grid is $120 \times 80 \times 20 \times 10 = 60{,}000$. Each grid point represents a specific group of data with the given temperature, pressure, feed gas flow rate, and H_2 to N_2 ratio. All these data points are fed to the trained SMOTE-integrated NNs model (4-input 1-output) to predict the associated NH_3 concentration. The index of input reaction conditions is

then located which leads to the maximum output NH_3 concentration. The resulting optimal temperature, pressure, feed gas flow rate, and H_2:N_2 ratio are 597.37 K, 0.55 MPa, $1.67 \times 10^{-3}\ m^3/s\,kg_{cat}$, and 1 respectively. Compared with Figure 2, the optimal microwave-assisted ammonia synthesis reaction conditions identified by the SMOTE-integrated NNs model are consistent with the experimental results. The four-input one-output model is used here because the design optimization problem requires the simultaneous consideration of all four design variables (i.e., temperature, pressure, feed flow rate, and hydrogen to nitrogen ratio). Despite the fact that the two-input model shows better performance than the four-input model as presented in the previous section, the two-input model is derived by varying only two of these variables while fixing the other two. It does not provide a holistic optimization addressing all the experimental operating conditions.

At the optimal reaction condition, we perform a check on if the physical behaviors are correctly captured based on prior experimental knowledge. Detailed information is provided in Section A of Appendix S1. We also emphasize the importance to verify the "gradient" around the optimal solution based on prior experimental knowledge. To give a more intuitive idea, Figure 11 shows the results when the NNs model is trained using SMOTE synthetic data and duplicate experimental data. The duplication of experimental data refers to repeating the 46 original data and mix with the synthetic data. This can contribute to balance the number of real experimental data and synthetic data in the NN training dataset (e.g., 50% vs. 50%). As shown in Figure 11A, the resulting discrete and continuous predictions are both satisfactory. However, the simulation-based optimization identifies the optimal reaction conditions at H_2:N_2 = 5, T = 607.45 K, P = 0.55 MPa, and $F = 1.67 \times 10^{-3}\ m^3/s\,kg_{cat}$. Based on experimental results (Figure 2), this H_2 to N_2 ratio is expected to provide the lowest NH_3concentration compared with other ratio values. By checking the gradient around this "optimal" solution as depicted in Figure 11B, H_2:N_2 = 1 is correctly captured as a local extreme. However, the NNs model captures a monotonically increasing trend of NH_3 concentration around H_2:N_2 = 5 which renders this ratio a better solution. Given this, we deduce that the NNs model encounters overfitting due to the use of duplicate experimental data. This is quantitatively justified by comparing that training accuracy (98%) is higher than the validation accuracy (96%). This also explains why all the reported results in the previous sections utilize a large number of synthetic data (e.g., 40,635) but only appending the original 46 experimental data.

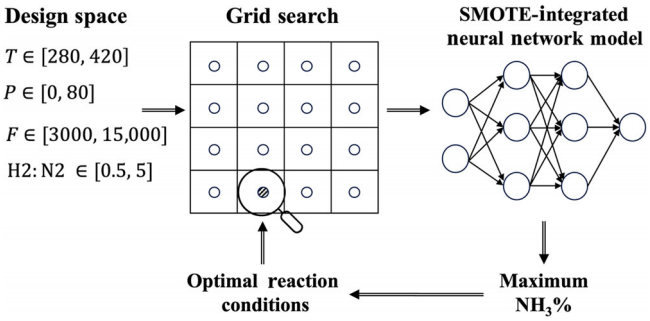

FIGURE 10 Optimization of reaction conditions.

3.5 | Comparison with other regression approaches

In what follows, we compare the proposed SMOTE-integrated NNs approach with other ML-aided regression methods. We also address the following key questions on: (i) why generating SMOTE synthetic

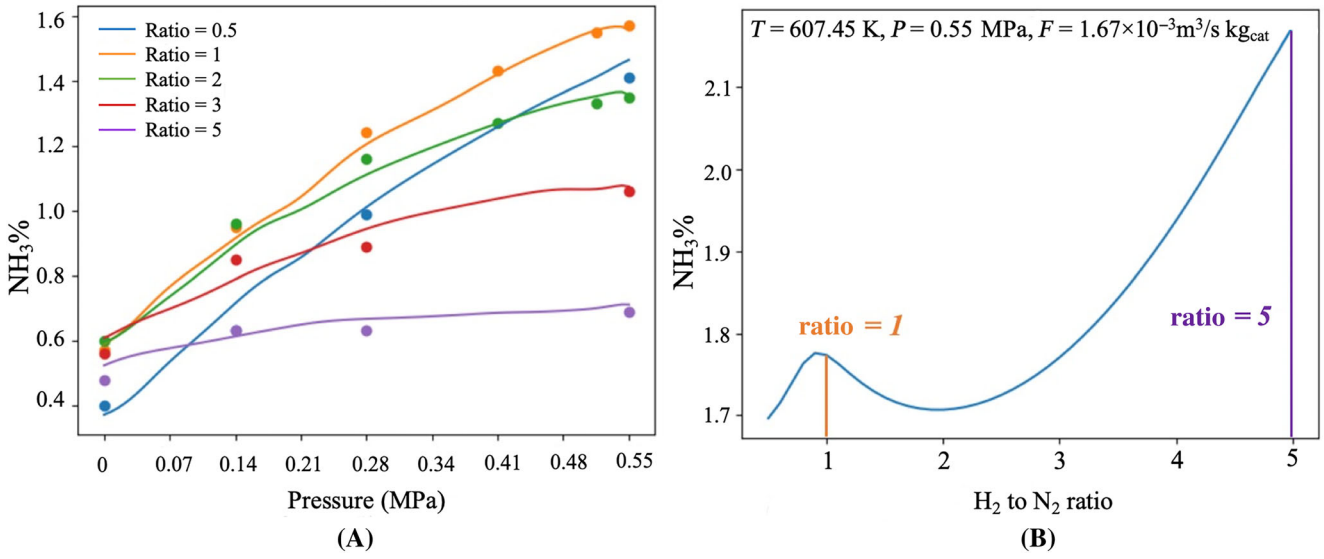

FIGURE 11 A scenario of prior physical knowledge violation. Markers: Original experimental data. Lines: synthetic minority oversampling technique (SMOTE)-integrated neural networks modeling. (A) Continuous prediction; (B) Impact of H_2 to N_2 ratio on optimal condition.

data instead of directly using the original limited experimental data as reported in many other works? (ii) why only validating discrete prediction is not sufficient?

3.5.1 | SMOTE-integrated linear regression

The linear regression model is fitted using the synthetic 23,000 unique datasets from SMOTE regression along with the 46 experimental data with an average accuracy of 83.54% for discrete prediction. The limited experimental data set is still split to 80% training data and 20% test data.

3.5.2 | SMOTE-integrated support vector regression

SVR is applied to model the microwave reactor using the synthetic 23,000 unique data points from SMOTE regression along with the 46 experimental data. The split of training and testing data are kept at 80% and 20%, respectively. RBF is found to be the best kernel function compared with linear and polynomial functions. The regularization parameter takes a value of 10. The average accuracy of SVR for discrete prediction is 84.22%, which is only slightly higher than the above linear regression model.

3.5.3 | NNs regression (without SMOTE)

In the previous sections of this article, we have demonstrated the potential and efficacy of SMOTE-integrated NNs modeling with application to this microwave-assisted ammonia synthesis reactor. Herein, we compare NNs modeling based on the 46 experimental data without SMOTE synthetic data. 80% data are fed to train the NNs and the rest 20% data are used as testing data. A feedforward network is adopted in which the data is passed from the input layer through hidden layers to the output layer. A total of 211 neurons are involved in the network, with Softplus as the activation function and MSE as the loss function. The trained NNs model has an average accuracy of discrete prediction as 86.20%, which is notably inferior to SMOTE-integrated NN.

To summarize, we have demonstrated that the SMOTE-integrated NNs approach provides superior discrete and continuous prediction performance over other regression approaches. A summary of the discrete prediction performances is given in Table 3.

4 | SYSTEMS INTEGRATION AND ANALYSIS

The SMOTE-integrated NNs model also enables to investigate the integration of this microwave-assisted ammonia synthesis technology with existing ammonia production infrastructure. Systems-level analyses are essential to understand the required design retrofit to the existing process flowsheets in order to incorporate the new processing pathways.[43] The quantitative evaluation on key process performance metrics (e.g., productivity, economics, sustainability) also aids to identify the bottlenecks toward the commercial deployment of these new technologies. In this section, we prove the concept that how the SMOTE-integrated NNs model can serve the purpose to systematically benchmark the microwave reactor with other alternative technologies (e.g., Haber-Bosch reactor) and up/downstream process sections.

We leverage the superstructure-based approach for process modeling and representation,[1,44] which can simultaneously account for multiple process design alternatives including their interactions and trade-offs. An indicative superstructure network is shown in Figure 12. The major process sections include: (i) nitrogen production via air separation unit (ASU), (ii) hydrogen production using water electrolyzer and/or integrated methane steam reforming and water gas shift (MSR-WGS), (iii) ammonia production via Haber-Bosch reactor and/or microwave reactor, and (iv) separations via a train of distillation columns and/or membranes. The ASU simulation flowsheet in Aspen Plus is given in Figure 13 as an example. This proof-of-the-concept superstructure comprises both the well-established commercial process technologies and the novel ones yet at the early development stage, thus enabling to assess their implementation and integration using a unified modeling framework. Future work will extend the superstructure for a holistic consideration of promising/sustainable process alternatives, such as to include membrane-based nitrogen separation from air.

For the superstructure modeling, the microwave reactor is described via the four-input one-output SMOTE-integrated NNs model obtained from Section 3.3.2. Mechanistic simulation models are developed for the other process technologies in Aspen Plus (ASU,[45] MSR-WGS,[46] Haber-Bosch,[46] distillations[46]) and Python (electrolyzer[47]) following the cited references. Data-driven surrogate models are then developed in Python for each of these process technologies to reduce the computational complexity while retaining sufficient modeling accuracy.[5] All the data-driven models are integrated to model the entire superstructure network (Figure 12) using the Python

TABLE 3 Summary–average accuracy for discrete prediction.

Method	SMOTE-integrated neural networks	Neural networks	SMOTE-integrated SVR	SMOTE-integrated linear regression
Average accuracy	96.10%	86.20%	84.22%	83.54%

Note: Discrete prediction accuracy is calculated based on the combined data points.
Abbreviations: SMOTE, synthetic minority oversampling technique; SVR, support vector regression.

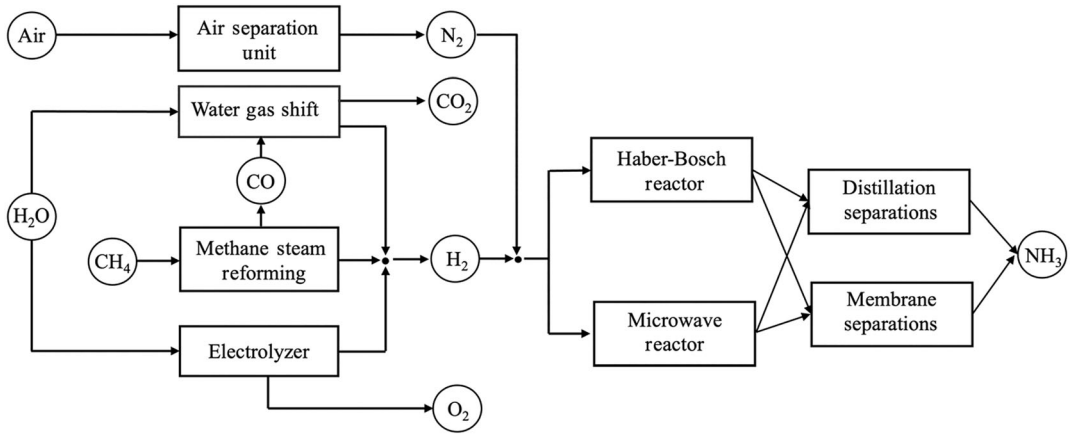

FIGURE 12 Systems integration—Superstructure for ammonia production.

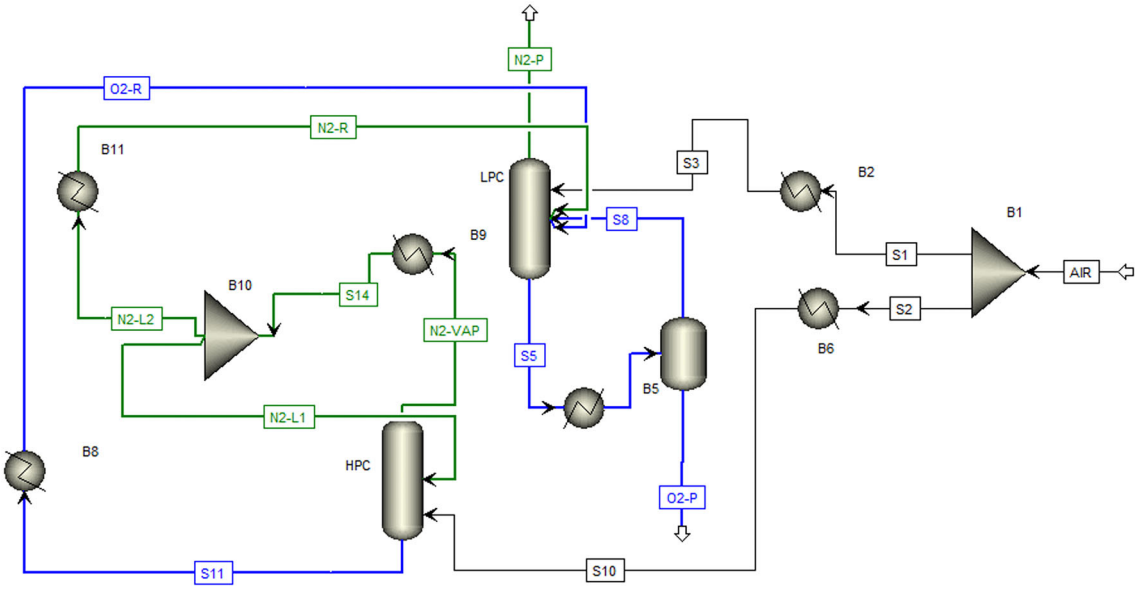

FIGURE 13 Cryogenic air separation unit — Aspen simulation set up.

platform. Mathematical optimization (e.g., mixed-integer nonlinear optimization) can thus be performed to investigate the selection of individual or hybrid production routes with different flowsheet design objectives.[46,48] To prove the concept, the simulation of two candidate routes is presented in Figure 14. Ongoing work focuses on performing comprehensive process synthesis optimization studies to investigate the integration of microwave-assisted ammonia synthesis for commercial ammonia production deployment with cost, energy, and sustainability considerations.

5 | CONCLUDING REMARKS

ML-aided approaches provide an instrumental tool to accelerate the research development and commercial deployment of novel intensified and sustainable process technologies. Key contributions of this work include: (i) Developing a SMOTE-integrated NNs approach for process-agnostic data-driven modeling based on limited experimental data, (ii) Applying for the continuous design optimization of a novel intensified microwave-assisted ammonia synthesis reactor, (iii) Demonstrating the potential to quantitatively evaluate the integration of microwave-assisted reactor for systems-level ammonia production starting from the early experimental development stage. More specifically, the SMOTE-integrated NN approach utilizes the synthetic minority over-sampling technique to address the limited data challenge by generating well-distributed synthetic data to enrich the ML training dataset and mitigate potential biases. The incorporation of NNs with soft plus activation function captures the nonlinear relationships between the process variables and target output. The resulting data-driven model has been applied to identify the optimal reaction conditions, which are proven to be consistent with experimental observations. On this basis, the hybrid modeling of

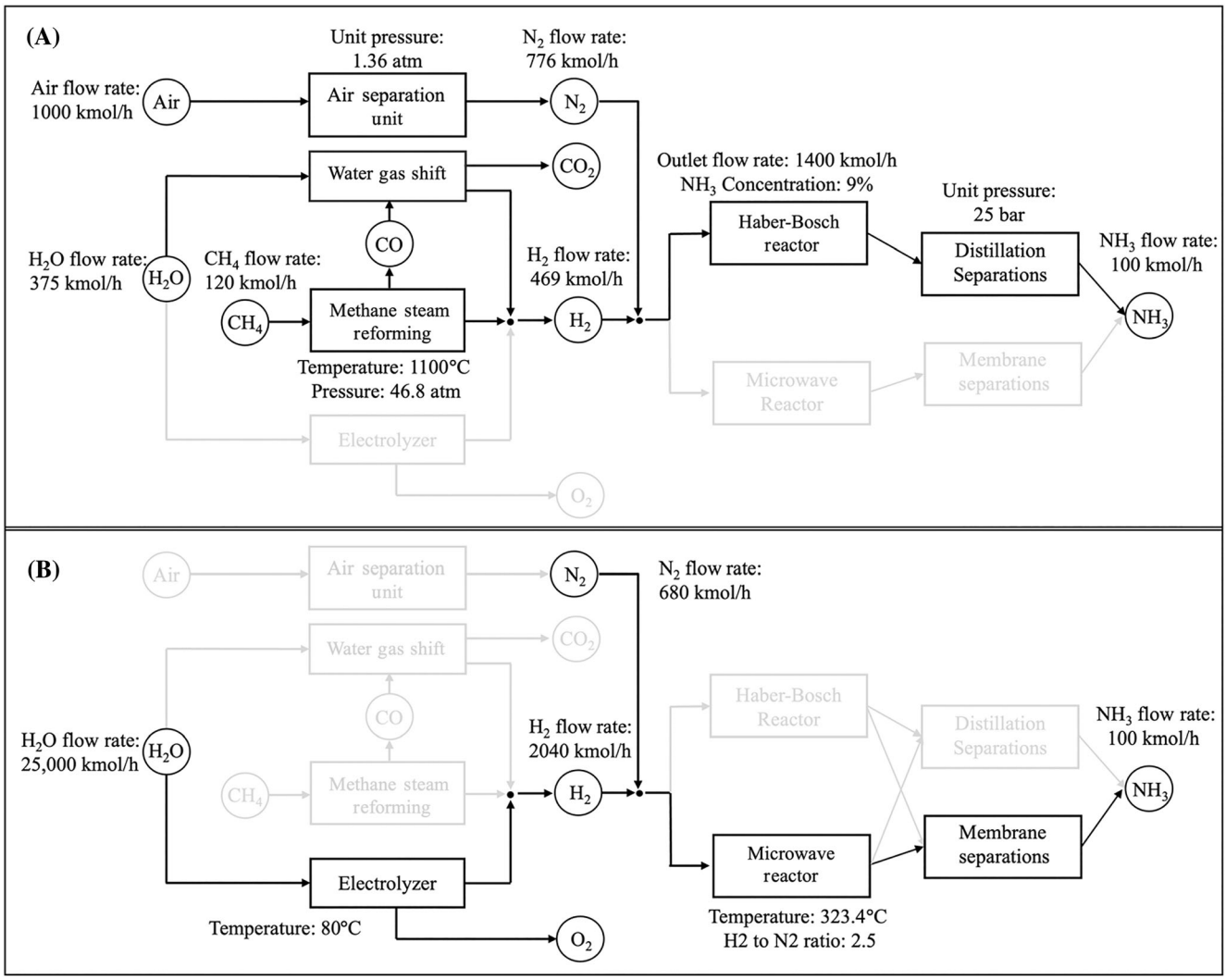

FIGURE 14 Systems integration—Simulation of candidate production routes. (A) Production route 1; (B) Production route 2.

microwave-assisted reaction systems via physics-informed ML presents a promising future area of research. The key research question is how to model the process more accurately by augmenting a limited amount of experimental data with first-principle models despite modeling simplifications/assumptions. Generative AI and large language models[49,50] also opens up exciting opportunities for data collection from all open literature, intelligent modeling building, and multiscale systems optimization.

AUTHOR CONTRIBUTIONS

Md Abdullah Al Masud: writing – original draft; methodology; software; formal analysis; validation; investigation. **Alazar Araia:** methodology; validation; formal analysis; writing – review and editing. **Yuxin Wang:** writing – review and editing; validation; methodology; conceptualization. **Jianli Hu:** writing – review and editing; conceptualization; methodology; validation. **Yuhe Tian:** writing – review and editing; conceptualization; methodology; software; validation; supervision.

ACKNOWLEDGMENTS

The authors acknowledge financial support from West Virginia University start-up funds and West Virginia Research Challenge Grant 23-009: Metal-Embedded Carbon-based Catalytic Membranes for co-Production of Ammonia and Ethylene.

DATA AVAILABILITY STATEMENT

The data that support the findings of this study are openly available in Github at https://github.com/masud045/SMOTE-Integrated-NNs, reference number DOI: 10.528/zenodo.11100144. Numerical data and open-source Python codes for Figures 4, 6–8, 10, 11, 13, and 14 are available in Appendix S1, corresponding to Sections A-H. In addition, the experimental data for Figure 2 are presented in Table 1.

ORCID

Jianli Hu https://orcid.org/0000-0003-3857-861X
Yuhe Tian https://orcid.org/0000-0001-7937-5785

REFERENCES

1. Pistikopoulos EN, Tian Y. Advanced Modeling and optimization strategies for process synthesis. *Annu Rev Chem Biomol Eng*. 2024;15:81-103.
2. Alshehri AS, Gani R, You F. Deep learning and knowledge-based methods for computer-aided molecular design – toward a unified approach: state-of-the-art and future directions. *Comput Chem Eng*. 2020;141:107005.
3. Lee JH, Shin J, Realff MJ. Machine learning: overview of the recent progresses and implications for the process systems engineering field. *Comput Chem Eng*. 2018;114:111-121.
4. Daoutidis P, Lee JH, Rangarajan S, et al. Machine learning in process systems engineering: challenges and opportunities. *Comput Chem Eng*. 2023;181:108523. https://www.sciencedirect.com/science/article/pii/S0098135423003939
5. Henao CA, Maravelias CT. Surrogate-based superstructure optimization framework. *AIChE J*. 2011;57(5):1216-1232.
6. Bradley W, Kim J, Kilwein Z, et al. Perspectives on the integration between first-principles and data-driven modeling. *Comput Chem Eng*. 2022;166:107898.
7. Raissi M, Perdikaris P, Karniadakis GE. Physics-informed neural networks: a deep learning framework for solving forward and inverse problems involving nonlinear partial differential equations. *J Comput Phys*. 2019;378:686-707.
8. Li J, Lim K, Yang H, et al. AI applications through the whole life cycle of material discovery. *Matter*. 2020;3(2):393-432.
9. Cao B, Adutwum LA, Oliynyk AO, et al. How to optimize materials and devices via design of experiments and machine learning: demonstration using organic photovoltaics. *ACS Nano*. 2018;12(8):7434-7444.
10. Lujan-Moreno GA, Howard PR, Rojas OG, Montgomery DC. Design of experiments and response surface methodology to tune machine learning hyperparameters, with a random forest case-study. *Expert Syst Appl*. 2018;109:195-205.
11. Lih WC, Bukkapatnam ST, Rao P, Chandrasekharan N, Komanduri R. Adaptive neuro-fuzzy inference system modeling of MRR and WIWNU in CMP process with sparse experimental data. *IEEE Trans Autom Sci Eng*. 2008;5(1):71-83.
12. Liu X, Xu Y, Li J, et al. A robust low data solution: dimension prediction of semiconductor nanorods. *Comput Chem Eng*. 2021;150:107315.
13. Chawla NV, Bowyer KW, Hall LO, Kegelmeyer WP. SMOTE: synthetic minority over-sampling technique. *J Artif Intell Res*. 2002;16:321-357.
14. Ramentol E, Caballero Y, Bello R, Herrera F. SMOTE-RSB*: a hybrid preprocessing approach based on oversampling and undersampling for high imbalanced data-sets using smote and rough sets theory. *Knowl Inform Syst*. 2012;33:245-265.
15. Kim HW, Lee SW, Na GS, et al. Reaction condition optimization for non-oxidative conversion of methane using artificial intelligence. *React Chem Eng*. 2021;6(2):235-243.
16. Mallapragada DS, Dvorkin Y, Modestino MA, et al. Decarbonization of the chemical industry through electrification: barriers and opportunities. *Joule*. 2023;7(1):23-41.
17. Bollini P, Diwan M, Gautam P, et al. Vision 2050: reaction engineering roadmap. *ACS Eng Au*. 2023;3(6):364-390.
18. Tian Y, Demirel SE, Hasan MF, Pistikopoulos EN. An overview of process systems engineering approaches for process intensification: state of the art. *Chem Eng Process Process Intens*. 2018;133:160-210.
19. Horikoshi S, Serpone N. General introduction to microwave chemistry. *Microwaves Catal Methodol Appl*; 2015:1-28.
20. Palma V, Barba D, Cortese M, Martino M, Renda S, Meloni E. Microwaves and heterogeneous catalysis: a review on selected catalytic processes. *Catalysts*. 2020;10(2):246.
21. Priecel P, Lopez-Sanchez JA. Advantages and limitations of microwave reactors: from chemical synthesis to the catalytic valorization of biobased chemicals. *ACS Sustainab Chem Eng*. 2018;7(1):3-21.
22. Muley PD, Wang Y, Hu J, Shekhawat D. *Microwave-Assisted Heterogeneous Catalysis*. Royal Society of Chemistry; 2021.
23. Melkote SG, Muley P, Dutta B, Wildfire C, Weiss R, Hu J. Developing a microwave-driven reactor for ammonia synthesis: insights into the unique challenges of microwave catalysis. *Cat Sci Technol*. 2023;13(8):2393-2406.
24. Wang Y, Khan TS, Wildfire C, Shekhawat D, Hu J. Microwave-enhanced catalytic ammonia synthesis under moderate pressure and temperature. *Cat Com*. 2021;159:106344.
25. Appl M. *The Haber-Bosch Heritage: The Ammonia Production Technology*. Vol 25. Fertilizer.org; 1997.
26. Goyal H, Chen TY, Chen W, Vlachos DG. A review of microwave-assisted process intensified multiphase reactors. *Chem Eng J*. 2022;430:133183.
27. Lakerveld R, Sturm GS, Stankiewicz AI, Stefanidis GD. Integrated design of microwave and photocatalytic reactors. Where are we now? *Curr Opin Chem Eng*. 2014;5:37-41.
28. Harrison A, Whittaker A. *Microwave Heating*. RSC Publishing; 2003.
29. Kulkarni A, Mishra G, Palla S, Ramesh P, Surya DV, Basak T. Advances in computational fluid dynamics Modeling for biomass pyrolysis: a review. *Energies*. 2023;16(23):7839.
30. Mevawala C, Bai X, Bhattacharyya D, Hu J. Dynamic data reconciliation, parameter estimation, and multi-scale, multi-physics modeling of the microwave-assisted methane dehydroaromatization process. *Chem Eng Sci*. 2021;239:116624.
31. Bai X, Muley PD, Musho T, et al. A combined experimental and modeling study of microwave-assisted methane dehydroaromatization process. *Chem Eng J*. 2022;433:134445.
32. Martínez González A, Stankiewicz A, Nigar H. Catalyst heating characteristics in the traveling-wave microwave reactor. *Catalysts*. 2021;11(3):369.
33. Wang Y, Wildfire C, Khan TS, et al. Effects of support and promoter on Ru catalyst activity in microwave-assisted ammonia synthesis. *Chem Eng J*. 2021;425:130546.
34. Torgo L, Ribeiro RP, Pfahringer B, Branco P. Smote for Regression. In: Correia L, Reis LP, Cascalho J, eds. *EPIA 2013*. Springer; 2013:378-389.
35. Mehlig B. *Machine Learning with Neural Networks: an Introduction for Scientists and Engineers*. Cambridge University Press; 2021.
36. Goel A, Goel AK, Kumar A. The role of artificial neural network and machine learning in utilizing spatial information. *Spat Inf Res*. 2023;31(3):275-285.
37. Getting PA. Emerging principles governing the operation of neural networks. *Annu Rev Neurosci*. 1989;12(1):185-204.
38. Nematzadeh S, Kiani F, Torkamanian-Afshar M, Aydin N. Tuning hyperparameters of machine learning algorithms and deep neural networks using metaheuristics: a bioinformatics study on biomedical and biological cases. *Comput Biol Chem*. 2022;97:107619.
39. Rasamoelina AD, Adjailia F, Sinčák P. A review of activation function for artificial neural network. *2020 IEEE 18th World Symposium on Applied Machine Intelligence and Informatics (SAMI)*. IEEE; 2020:281-286.
40. Rittig JG, Felton KC, Lapkin AA, Mitsos A. Gibbs–Duhem-informed neural networks for binary activity coefficient prediction. *Dig Dis*. 2023;2(6):1752-1767.
41. Montgomery DC, Peck EA, Vining GG. *Introduction to Linear Regression Analysis*. John Wiley & Sons; 2021.
42. Smola AJ, Schölkopf B. A tutorial on support vector regression. *Stat Comput*. 2004;14:199-222.
43. Cresko J, Rightor E, Carpenter A, et al. DOE industrial decarbonization roadmap. Technical Report. USDOE Office of Energy Efficiency and Renewable Energy (EERE). 2022:DOE/EE-2635.

44. Mencarelli L, Chen Q, Pagot A, Grossmann IE. A review on superstructure optimization approaches in process system engineering. *Comput Chem Eng*. 2020;136:106808.
45. Cheng M, Verma P, Yang Z, Axelbaum RL. Flexible cryogenic air separation unit—an application for low-carbon fossil-fuel plants. *Sep Purif Technol*. 2022;302:122086.
46. Demirhan CD, Tso WW, Powell JB, Pistikopoulos EN. Sustainable ammonia production through process synthesis and global optimization. *AIChE J*. 2019;65(7):e16498.
47. Sánchez M, Amores E, Abad D, Rodríguez L, Clemente-Jul C. Aspen plus model of an alkaline electrolysis system for hydrogen production. *Int J Hydrogen Energy*. 2020;45(7):3916-3929.
48. Niziolek AM, Onel O, Tian Y, Floudas CA, Pistikopoulos EN. Municipal solid waste to liquid transportation fuels–part iii: an optimization-based nationwide supply chain management framework. *Comput Chem Eng*. 2018;116:468-487.
49. Decardi-Nelson B, Alshehri AS, Ajagekar A, You F. Generative Ai and process systems engineering: the next frontier. *Comput Chem Eng*. 2024;187:108723.
50. Ashraf C, Joshi N, Beck DA, Pfaendtner J. Data science in chemical engineering: applications to molecular science. *Annu Rev Chem Biomol Eng*. 2021;12(1):15-37.

SUPPORTING INFORMATION

Additional supporting information can be found online in the Supporting Information section at the end of this article.

How to cite this article: Masud MAA, Araia A, Wang Y, Hu J, Tian Y. Machine learning-aided process design using limited experimental data: A microwave-assisted ammonia synthesis case study. *AIChE J*. 2024;e18621. doi:10.1002/aic.18621